Soliton Waves and Breather Waves to the (2+1)-Dimensional Boussinesq Equation

Chun-Xue Zhao

Abstract— **The (2+1) Boussinesq equation is widely used in fluid dynamics, particularly in the study of shallow water waves and other wave phenomena. In this work, we utilize Hirota's bilinear method to explore soliton waves, breather waves and their dynamic mechanisms to (2+1)-dimensional Boussinesq equation. These findings may contribute to a deeper understanding of high-dimensional nonlinear wave phenomena.**

Keywords: (2+1)-dimensional Boussinesq equation, Hirota bilinear, soliton waves, breather waves

1 Introduction

Nonlinear evolution equations (NLEEs) are fundamental to understanding complex physical phenomena across various disciplines, including physics, biology, chemistry, and mechanics. Obtaining exact solutions to these NLEEs is essential for unraveling the underlying mechanisms of such phenomena and has become one of the most significant challenges in scientific research.

Exact wave solutions to NLEEs and their generalized forms are indispensable for studying complex physical phenomena and addressing nonlinear engineering problems [1, 2]. Constructing these wave solutions is of great importance for scientific and engineering applications. Over time, numerous systematic methods have been established to effectively tackle NLEEs. These methods include Lie group method [3], Darboux transformation [4], inverse scattering method [5], Bäcklund transformation method [6], the Hirota bilinear method [7], KP hierarchy reduction method [8, 9], and other advanced techniques [10, 11]. These approaches have significantly advanced the ability to analyze and solve nonlinear systems.

In the present work, we explore the exact wave solutions of the following (2+1)-dimensional Boussinesq equation using Hirota bilinear method.

$$u_{tt} - u_{xx} - u_{yy} - (u^2)_{xx} = 0. \tag{1.1}$$

This study proceeds as follows: in section 2, we apply the Hirota's bilinear method to derive a new bilinear form and construct soliton wave solutions. Section 3 devotes to the construction of new breather wave solutions. In section 4, we summarize the main findings of this study and discuss their potential implications for future research.

2 The soliton wave solutions

Based on the transformation $u = 6(\ln f)_{xx}$, we get the bilinear form of Eq.(1.1) as follows

$$(D_t^2 - D_x^2 - D_x^4 - D_y^2) f \cdot f = 0, \tag{2.1}$$

where D represents the Hirota bilinear operator defined as

$$\begin{aligned} D_\mu^m D_\nu^n \alpha_1 \cdot \alpha_2 = (\frac{\partial}{\partial \mu} - \frac{\partial}{\partial \mu'})^m (\frac{\partial}{\partial \nu} - \frac{\partial}{\partial \nu'})^n \alpha_1(\mu, \nu) \\ \cdot \alpha_2(\mu', \nu')|_{\mu'=\nu, \mu'=\nu}, \end{aligned} \tag{2.2}$$

where $\alpha_1, \alpha_2 \in C^\infty(R^2)$. Following Hirota bilinear method, the N-soliton wave solutions to Eq.(1.1) is obtained by

$$\begin{aligned} &u = 6(\ln f)_{xx}, \\ &f = \sum_{\zeta=0,1} \exp(\sum_{j=1}^{N} \zeta_i \eta_i + \sum_{1 \le i < j \le N} \zeta_i \zeta_j A_{ij}), \\ &\eta_i = a_i(x + b_i y + c_i t) + \gamma_i, \\ &c_i^2 = a_i^2 + b_i^2 + 1, \\ &\exp(A_{ij}) = -\frac{B_{ij}}{C_{ij}}, \end{aligned} \tag{2.3}$$

where $a_i, b_i, \gamma_i (i = 1, 2, \ldots, N)$ are arbitrary real constants and $\sum_{\zeta=0,1}$ is the summation that takes over all possible combinations of $\zeta_i, \zeta_j = 0, 1 (i, j = 1, 2, \ldots N)$,

$$\begin{aligned} B_{ij} &= (a_i - a_j)^4 + (a_i - a_j)^2 + (a_i b_i - a_j b_j)^2 \\ &\quad - (a_i c_i - a_j c_j)^2, \\ C_{ij} &= (a_i + a_j)^4 + (a_i + a_j)^2 + (a_i b_i + a_j b_j)^2 \\ &\quad - (a_i c_i + a_j c_j)^2. \end{aligned} \tag{2.4}$$

Let N=1, we gain the one-soliton solution of Eq.(1.1) by

$$u = 6(\ln(1 + e^\eta))_{xx}, \tag{2.5}$$

where $\eta = a_1(x + b_1 y + c_1 t) + \gamma_1$, and a_1, b_1, γ_1 are arbitrary constants.

Let $N = 2$, the two-soliton wave solution of Eq.(1.1) is

$$u = 6(\ln(1 + e^{\eta_1} + e^{\eta_2} + e^{\eta_1 + \eta_2 + A_{12}}))_{xx}, \tag{2.6}$$

Manuscript received May 13, 2025; revised July 31, 2025.

Chun-Xue Zhao is a lecturer of School of Mathematics and Statistics, Anyang Normal University, Anyang 455000, PR China (corresponding author to provide phone: +86 1536696223; fax: +86 1536696223; e-mail: zhaochunxue66@163.com).

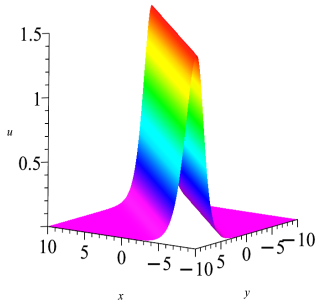

Figure 1: Single soliton solution with parameters: $a_1 = 1, b_1 = 1, \gamma_1 = 0, t = 0$.

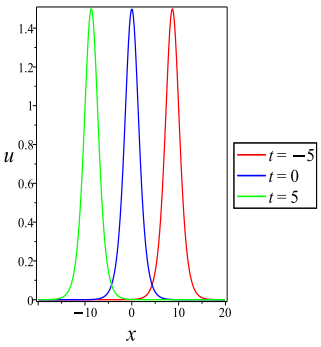

Figure 2: Cross-sectional graphs at $t = -5, 0, 5$, respectively.

where $\eta_i (i = 1, 2), \exp(A_{ij}) (i = 1, j = 2)$ are are consistent with the result in Eq.(2.3).

In the following, we represent these two soliton wave solutions in Figs.1-6. In Figs.1-2, it is observed that the amplitude and width of the one-soliton remain constant during propagation. This suggests that there is neither energy loss nor gain as the soliton moves, underscoring its stability. The figures also illustrate that the amplitudes of the excited states are constrained and nearly equal across various spatial positions. This implies a uniform energy distribution of the excited states, which is maintained by the stability of the soliton. Although minor variations in the state of the soliton may occur at different times and locations, its amplitude remains predominantly consistent throughout the spatial domain, reinforcing the stability of the solution. In Fig.3, the shape of the double soliton solution is depicted, with the overhead view and contour plot shown in Figs.4-5. Fig.6 displays the cross-sections of the two solitons at different positions. The coordinates of the points corresponding to the amplitudes of the two solitons before and after the collision are (-5.547, 0.375), (5.739, 0.375), (-10.25, 0.539), and (11.006, 0.539), respectively. These results confirm that both solitons preserve their amplitudes during the collision process. The collision point of the two solitons is located at (0, 1.012), indicating that the amplitude at the collision point does not equal the sum of the amplitudes of the two interacting solitons. The configuration of the double soliton solutions for $t = -8$ and $t = 8$ is represented in Figs.7-8, respectively. It is evident from these figures that the structural shape of the soliton waves remains consistent, with only the position changing, thus illustrating the characteristic behavior of soliton waves.

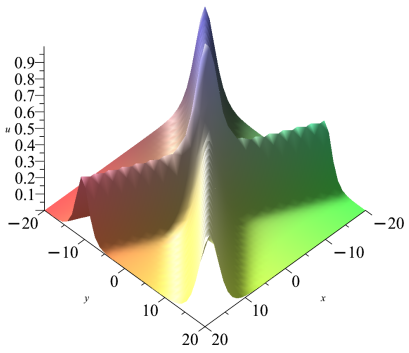

Figure 3: Double soliton solution with parameters: $a_1 = 0.5, a_2 = 0.6, b_1 = 2, b_2 = -1, \gamma_1 = 0, \gamma_2 = 0, t = 0$.

3 Breather wave solutions

To get the two-order breather wave solution, the preliminary assumption is

$$f = 1 + \varepsilon(e^{\xi_1} + e^{\xi_2}) + \varepsilon^2 e^{\xi_1 + \xi_2 + A_{12}}, \qquad (3.1)$$

where

$$\begin{aligned} \xi_1 &= k_1 x + w_1 y + p_1 t + \phi_1, \\ \xi_2 &= k_2 x + w_2 y + p_2 t + \phi_2. \end{aligned} \qquad (3.2)$$

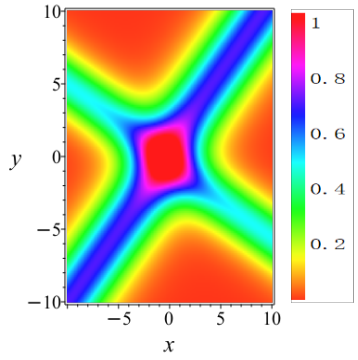

Figure 4: Density plot of double soliton solution.

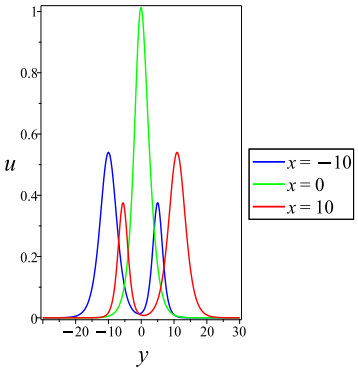

Figure 6: Cross-sectional graphs at $x = -10, 0, 10$, respectively.

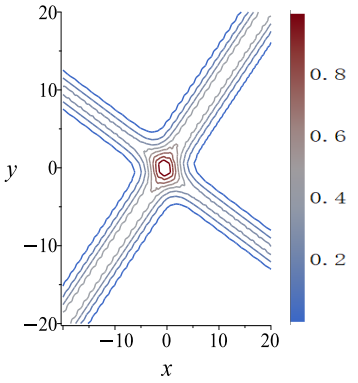

Figure 5: Contour plot of double soliton solution.

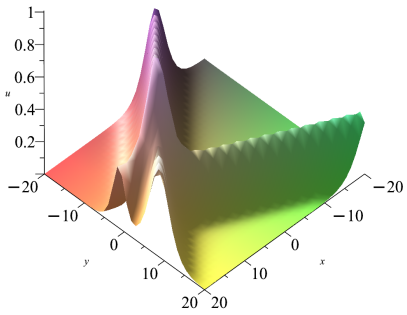

Figure 7: Double soliton solution with parameters: $t = -8$.

Substituting Eq.(3.1) into Eq.(2.1), the coefficients of each power of ε are set to zero, it yields

$$e^{A_{12}} = -\frac{E}{F},$$
$$w_i^2 = p_i^2 - k_i^2 - k_i^4 (i = 1, 2), \tag{3.3}$$

where

$$E = (k_1 - k_2)^4 + (k_1 - k_2)^2 + (w_1 - w_2)^2 - (p_1 - p_2)^2,$$
$$F = (k_1 + k_2)^4 + (k_1 + k_2)^2 + (w_1 + w_2)^2 - (p_1 + p_2)^2.$$

Extending the parameters to complex values, we study the case of complex-conjugate pairs from the original real parameters in (3.1) as follows

$$k_1 = k_2^* = ik, p_1 = p_2 = p, \phi_1 = \phi_2 = \phi, \tag{3.4}$$

at this point, we have

$$w_1 = w_2 = w = \sqrt{p^2 + k^2 - k^4},$$
$$\xi_1 = ikx + wy + pt + \phi,$$
$$\xi_2 = -ikx + wy + py + \phi, \tag{3.5}$$

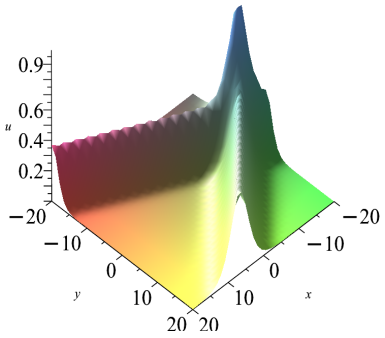

Figure 8: Double soliton solution with parameters: $t = 8$.

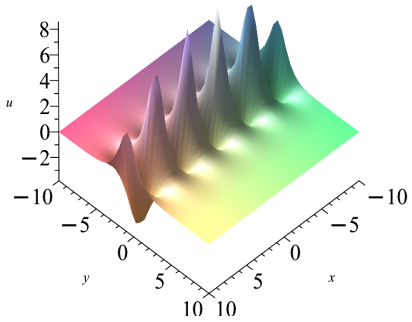

Figure 9: Breather-wave solution with parameters: $k = \frac{3}{2}, p = 2, t = 0$.

then, we can get

$$\begin{aligned} f &= 1 + e^{\xi_1} + e^{\xi_2} + e^{\xi_1+\xi_2+A_{12}} \\ &= 1 + e^{wy+pt+\phi}(e^{ikx} + e^{-ikx}) + e^{2wy+2pt+2\phi} \cdot e^{A_{12}} \\ &= 1 + 2e^{wy+pt+\phi}\cos(kx) + e^{2wy+2pt+2\phi} \cdot e^{A_{12}} \\ &\sim \sqrt{H}\cosh(wy + pt + \phi + \ln(\sqrt{H})) + \cos(kx), \quad (3.6) \end{aligned}$$

where

$$H = e^{A_{12}} = \frac{4k^2 - 1}{k^2 - 1}.$$

Substituting Eq(3.6) into $u = 6(\ln f)_{xx},$, we get the breather wave solution as follows

$$u = -\frac{6k^2\cos(kx)}{G} - \frac{6k^2\sin(kx)^2}{G^2}, \qquad (3.7)$$

where

$$G = \sqrt{H}\cosh(\sqrt{-k^4 + k^2 + p^2}y + pt + \frac{\ln H}{2}) + \cos(kx).$$

Figs.9-11 depict the morphological structure of breather waves, their overhead view, and contour plot, corresponding to the parameters $k = \frac{3}{2}$, $p = 2$, and $t = 0$, respectively. The figures indicate that breather wave solutions are localized. In addition, it is demonstrated that breathers undergo periodic amplitude modulation either in space or time, while maintaining their spatial confinement. The configuration of the breather waves for $t = -3$ and $t = 3$ is represented in Figs.12-13, respectively. It is evident from these figures that the structural shape and amplitude of the breather waves remains consistent, with only the position changing, thus illustrating the characteristic behavior of breather waves.

The methodology outlined above naturally extends to higher-order breather solutions. Beginning with an extended ε-expansion of f:

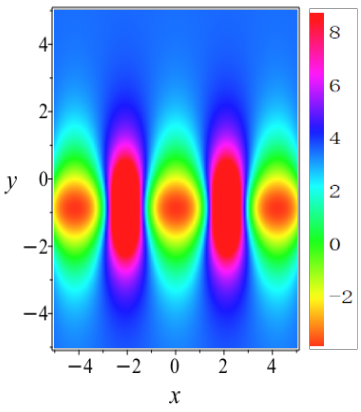

Figure 10: Density plot of breather-wave solution.

$$\begin{aligned} f = 1 &+ \varepsilon(e^{\xi_1} + e^{\xi_2} + e^{\xi_3}) + \varepsilon^2(e^{\xi_1+\xi_2+A_{12}} + e^{\xi_1+\xi_3+A_{13}} \\ &+ e^{\xi_2+\xi_3+A_{23}}) + \varepsilon^3 e^{\xi_1+\xi_2+\xi_3+A_{12}+A_{13}+A_{23}} + \ldots. \end{aligned} \qquad (3.8)$$

Substituting Eq.(3.8) into Eq.(2.1) yields a sequence of equations of different orders of ε, whose solution is

$$f = \sum_{\zeta=0,1} \exp(\sum_{i<j}^{(N)} \zeta_i\zeta_j A_{ij} + \sum_{j=1}^{N} \zeta_j\xi_j), \qquad (3.9)$$

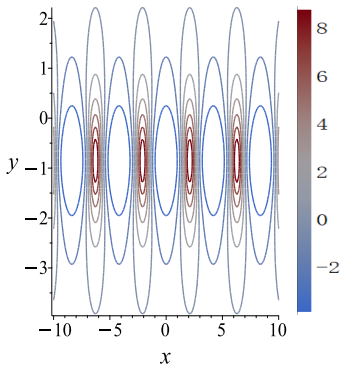

Figure 11: Contour plot of breather-wave solution.

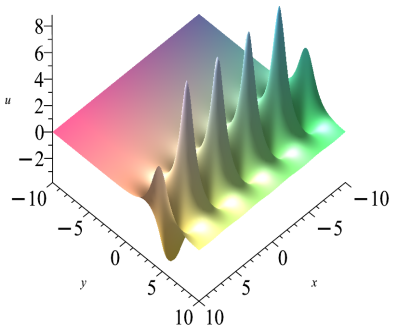

Figure 12: Breather-wave solution with parameters: $k = \frac{3}{2}, p = 2, t = -3$.

where

$$\begin{aligned} \xi_j &= k_j x + w_j y + p_j t + \phi_j, \\ e^{A_{ij}} &= -\frac{M_{ij}}{N_{ij}}, \\ w_i^2 &= p_i^2 - k_i^2 - k_i^4 (i = 1, 2, \ldots), \end{aligned} \tag{3.10}$$

in which k_i, p_i, w_i, ϕ_i are arbitrary complex constants, $\sum_{\zeta=0,1}$ indicates summation over all possible combinations of $\zeta_1 = 0, 1, \zeta_2 = 0, 1, \ldots, \zeta_N = 0, 1$; $\sum_{i<j}^{N}$ extends over all distinct pairs (i, j) where $i < j$, $M_{ij} = (k_i - k_j)^4 + (k_i - k_j)^2 + (w_i - w_j)^2 - (p_i - p_j)^2$, $N_{ij} = (k_i + k_j)^4 + (k_i + k_j)^2 + (w_i + w_j)^2 - (p_i + p_j)^2$.

As discussed in Ref. [12], by appropriate constraints

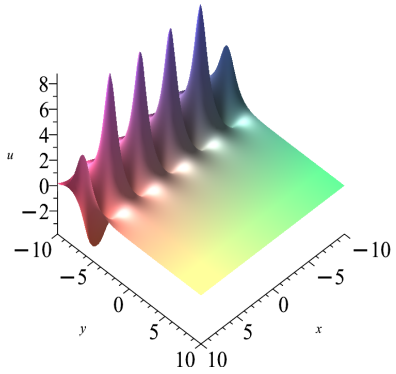

Figure 13: Breather-wave solution with parameters: $k = \frac{3}{2}, p = 2, t = 3$.

of k_i, w_i, p_i, ϕ_i in Eq. (3.8),

$$N = 2n, w_{n+i} = w_i^*, p_{n+i} = p_i^*, k_{n+i} = k_i^*, \phi_{n+i} = \phi_i^*, \tag{3.11}$$

at the same time, k_i must be pure imaginary numbers, w_i must be real numbers and these parameters satisfy $p_i^2 + k_i^2 - k_i^4 \geq 0$, With these conditions, the n-order breather wave solutions would be derived.

4 Conclusions

This study delves into the (2+1)-dimensional Boussinesq equation, a fundamental model in fluid dynamics crucial for representing shallow water waves and associated nonlinear phenomena. Utilizing the Hirota's bilinear method, we meticulously construct exact solutions, encompassing soliton and breather waves, and subsequently examine their interaction dynamics. Our findings elucidate the propagation mechanisms and stability attributes of these localized waves, providing a more profound comprehension of energy localization and the modulation instability in nonlinear systems.

References

[1] Wu, C.Q., Li, M.H., Luo, H., Hu, T., Yi, S.M. and Wang G.H., "Dynamic Response and Vibration Control of Deep-water Bridge Piers under Ship Wave Excitation," *Eng. Lett.*, vol. 33, no. 6, pp. 1871-1878, 2025.

[2] Saadeh, R., Unami, K., Qazza, A., Batiha, I.M. and Mohawesh, O., "Linear Fractional Differential Equations for Modeling Nonlinear Hydro Environmental Phenomena," *Eng. Lett.*, vol. 33, no. 6, pp. 1913-1918, 2025.

[3] Bluman, G.W. and Kumei, S., *Symmetries and Differential Equations*, Springer, Berlin, 1989.

[4] Matveev, V.B. and Salle, M.A., *Darboux Transformation and Solitons*, Springer, Berlin, 1991.

[5] Ablowitz, M.J., *Solitons, Nonlinear Evolution Equations and Inverse Scattering*, Cambridge University Press, Cambridge, 1992.

[6] Matsuno, Y., *Bilinear Transformation Method*, Academic, New York, 1984.

[7] Hirota, R., *The Direct Method in Soliton Theory*, Cambridge University Press, Cambridge, 2004.

[8] Jimbo, M. and Miwa, T., "Solitons and infinite dimensional Lie algebras," *Publ. Res. Inst. Math. Sci.*, vol. 19, no. 3, pp. 943-1001, 1983.

[9] Rao, J.G., Wang, L.H., Zhang, Y. and He, J.S., "Rational solutions for the Fokas systems," *Commun. Theor. Phys.*, vol. 64, no. 12, pp. 605-618, 2015.

[10] Ma, W.X., "Lump solutions to the Kadomtsev-Petviashvili equation," *Phys. Lett. A*, vol. 379, no. 36, pp. 1975-1978, 2015.

[11] Kheybari, S., Darvishi, M.T. and Wazwaz, A.M., "A semi-analytical algorithm to solve systems of integro-differential equations under mixed boundary conditions," *Appl. Math. Comput.*, vol. 317, pp. 72-89, 2017.

[12] Rao, J.G., Cheng, Y. and He, J.S., " Rational and semi-rational solutions ofthe nonlocal DaveyCStewartson equations," *Stud. Appl. Math.*, vol. 139, pp. 568-598, 2017.